

# Modeling high-dimensional dependence among astronomical data

R. Vio<sup>1</sup>, T.W. Nagler<sup>2</sup>, and P. Andreani<sup>3</sup>

<sup>1</sup> Chip Computers Consulting s.r.l., Viale Don L. Sturzo 82, S.Liberale di Marcon, 30020 Venice, Italy  
e-mail: robertovio@tin.it

<sup>2</sup> Mathematical Institute, Leiden University, Niels Bohrweg 1, 2333 CA Leiden  
e-mail: t.w.nagler@math.leidenuniv.nl

<sup>3</sup> ESO, Karl Schwarzschild strasse 2, 85748 Garching, Germany  
e-mail: pandrean@eso.org e-mail: pandrean@eso.org

Received....; accepted....

## ABSTRACT

Fixing the relationship among a set of experimental quantities is a fundamental issue in many scientific disciplines. In the two-dimensional case, the classical approach is to compute the linear correlation coefficient  $\rho$  from a scatterplot. This method, however, implicitly assumes a linear relationship between the variables. Such assumption is not always correct. With the use of the partial correlation coefficients, an extension to the multi-dimensional case is possible. However, the problem of the assumed mutual linear relationship among the variables still remains. A relatively recent approach which permits to avoid this problem is modeling the joint probability density function (PDF) of the data with copulas. These are functions which contain all the information on the relationship between two random variables. Although in principle this approach can work also with multi-dimensional data, theoretical as well computational difficulties often limit its use to the two-dimensional case. In this paper, we consider an approach, based on so-called vine copulas, which overcomes this limitation and at the same time is amenable to a theoretical treatment and feasible from the computational point of view. We apply this method to published data on the near-IR and far-IR luminosities and atomic and molecular masses of the Herschel Reference Sample. We determine the relationship among the luminosities and gas masses and show that the far-IR luminosity can be considered as the key parameter which relates all the other three galaxy properties. Once removed from the 4D relation, the residual relation among the other three is negligible. This may be interpreted as that the correlation between the gas masses and near-IR luminosity is driven by the far-IR luminosity, likely by the star-formation activity of the galaxy.

**Key words.** Methods: data analysis – Methods: statistical

## 1. Introduction

Modeling the relationship among a set of experimental quantities is not straightforward. Often no theoretical hints are available that would allow to fix the dependence among the involved variables. Hence, the work has to be entirely based on the analysis of the data. In the two-dimensional case, an example is represented by the scatterplots and the computation of the corresponding linear correlation coefficients  $\rho$ . Its extension to the multi-dimensional case is possible with the partial correlation coefficients. The main limitation of this approach is the implicit assumption of a linear relationship among the variables under study. This is often an unrealistic condition. For this reason, a relatively recent alternative consists in modeling the joint probability distribution function (PDF) of the data. However, this task is not trivial even in the two-dimensional case. Families of bivariate PDFs are available (Balakrishnan & Lai 2010), but are little flexible and difficult to use. Things worsen for the multi-dimensional case (Kotz et al. 2000). A relatively recent alternative is based on copulas. These are simply multivariate cumulative distribution functions (CDF) with standard uniform margins. They are used to describe the dependence between random variables, and their main role is to disentangle margins and the dependence structure (Nelsen 2006; Durante & Sempi 2016; Hofert et al. 2018). With copulas it is possible to decompose a joint probability distribution into their margins and a function which couples them. The copula is that coupling function.

In cosmology two-dimensional copulas have been used by Scherrer et al. (2010) for the determination of the PDF of the density field of large-scale structure of the Universe, by Lin & Kilbinger (2015) and Lin et al. (2016) to predict weak-lensing peak counts and by Sato et al. (2010, 2011) for the precise estimation of cosmological parameters. Other astronomical applications have been the determination of the far-ultraviolet and far-infrared bivariate luminosity function of galaxies (Takeuchi 2010; Takeuchi et al. 2011), the determination of the K-band and the sub-millimeter luminosity function (Andreani et al. 2014) and the bivariate luminosity vs. the mass functions of the local HRS galaxy sample (Andreani et al. 2018).

In principle the copula approach can work with multidimensional data but theoretical as well computational difficulties often limit its use to the two-dimensional case. Recently, however, vine copulas have been proposed in the statistical literature as an approach which overcomes this limitation and at the same time is amenable to a theoretical treatment and feasible from the computational point of view. The strength of vine copulas is that they allow, in addition to the separation of margins and dependence by the copula approach, tail asymmetries and separate multivariate component modeling. This is accommodated by constructing multivariate copulas using only bivariate building blocks, which can be selected independently. These building blocks are glued together to valid multivariate copulas by appropriate conditioning (Joe 2015; Czado 2019). This makes vine copulas a very

flexible and reliable tool even in the case of very high dimensional data.

In this paper we make use of multidimensional copulas, described in Secs. 2 and 3 and in particular of vine copulas, outlined in Sec. 4 and 5. We apply them to a data set related to a complete nearby sample of galaxies which has been observed at various wavelengths (Andreani et al. 2018, and references therein) and show its use to highlight the underline the relation among physical properties of the galaxies in Sec. 6.

## 2. What are copulas?

A  $d$ -dimensional copula  $C_{1,\dots,d}(\mathbf{u})$ ,  $\mathbf{u} \in [0, 1]^d$  is simply a multivariate CDF with standard uniform univariate margins. Its importance is due to the Sklar's theorem: for any  $d$ -dimensional CDF  $F(\mathbf{x})$ ,  $\mathbf{x} = (x_1, \dots, x_d) \in \mathbb{R}^d$ , with univariate margins  $F_1(x_1), \dots, F_d(x_d)$ , there exists a  $d$ -dimensional copula  $C_{1,\dots,d}(\mathbf{u}) : [0, 1]^d \rightarrow [0, 1]$  such that

$$F(\mathbf{x}) = C_{1,\dots,d}(F_1(x_1), \dots, F_d(x_d)) = C_{1,\dots,d}(u_1, \dots, u_d), \quad (1)$$

where  $u_1 = F_1(x_1), \dots, u_d = F_d(x_d)$ . The converse also holds, i.e. given a  $d$ -dimensional copula  $C_{1,\dots,d}(\mathbf{u})$  and univariate CDFs  $F_1(x_1), \dots, F_d(x_d)$ , the CDF  $F(\mathbf{x})$  defined by Eq. (1) is a  $d$ -dimensional CDF with margins  $F_1(x_1), \dots, F_d(x_d)$ . This means that copulas are those functions which combine the univariate margins  $F_1(x_1), \dots, F_d(x_d)$  to form the  $d$ -dimensional CDF  $F(\mathbf{x})$ . In other words, copulas link multivariate CDFs to their univariate margins. The importance of copula is more evident if the PDFs  $f(\mathbf{x})$  are considered. Indeed, it can be shown that

$$f(x_1, \dots, x_d) = c_{1,\dots,d}(F_1(x_1), \dots, F_d(x_d)) \cdot f_1(x_1) \cdots f_d(x_d), \quad (2)$$

where

$$c_{1,\dots,d}(u_1, \dots, u_d) = \frac{\partial^d C_{1,\dots,d}(u_1, \dots, u_d)}{\partial u_1 \cdots \partial u_d}. \quad (3)$$

From Eq. (2), any joint PDF  $f(\mathbf{x})$  can be factorized into the product of two terms. One is the product of the marginal PDFs  $\{f_i(x_i)\}$  and the other is the copula density  $c_{1,\dots,d}(\mathbf{u})$ . The first term provides information on the statistical properties of the individual random variables  $\{x_i\}$  whereas the second term provides information on their mutual dependence. Therefore, the importance of  $c_{1,\dots,d}(\mathbf{u})$  lies in the fact that it describes the dependence structure among the random variables in separation of the associated marginal PDFs.

If a set of  $n$   $d$ -dimensional random data  $\{\mathbf{x}_k\}$ ,  $k = 1, \dots, d$ , with  $\mathbf{x}_k = \{x_{t,k}\}$ ,  $t = 1, \dots, n$ , is available and the margins  $\{F_k(x_k)\}$  with the corresponding PDFs  $\{f_k(x_k)\}$  are known, the standard procedure to estimate  $f(x_1, \dots, x_d)$  is as follows: first, compute the standard uniform variates  $\mathbf{u}_k = F_k(\mathbf{x}_k)$ , then fit their joint distribution by a copula  $C_{1,\dots,d}(\mathbf{u}|\boldsymbol{\theta})$ , which belongs to a continuous parametric family with characteristic parameters  $\boldsymbol{\theta} = \{\theta_1, \dots, \theta_{n_p}\}$ . After that, Eq. (2) provides the joint PDF. A common method for fitting the copula is based on an estimate of the parameters  $\boldsymbol{\theta}$  through a maximum likelihood method, but other techniques are possible too (Hofert et al. 2018). Often, however, the margins are not available. In this case, an alternative is to fit each set  $\mathbf{x}_k$  with a PDF belonging to the Johnson, generalized Lambda or any other family of parametric PDFs (Balakrishnan & Lai 2010), to compute the uniform random variates  $\mathbf{u}_k = F_k(\mathbf{x}_k)$  and then, as before, to fit a copula. A variant is the computation of the random variates  $\mathbf{u}_k$  by means of the so called pseudo-observations  $u_{t,k} = R_{t,k}/(n+1)$  with  $R_{t,k}$  the rank of  $x_{t,k}$

among  $(x_{1,k}, \dots, x_{n,k})$ . Since in general, one has no indication of which kind of copula is suited for the data of interest, the typical solution is to fit a set of copulas and to choose that which provides the best result.

In principle, the above procedures can be applied to any  $d$ -dimensional data set. The point is that most of the parametric copula families available in literature are two-dimensional (e.g. see Joe 2015) and the few available for a multidimensional analysis are not flexible enough. An alternative approach based on a non-parametric copula estimate has been also proposed (e.g., Nagler & Czado 2016; Nagler et al. 2017).

## 3. Preliminary considerations

Given that most of the available copula families are two-dimensional, it is unclear how a  $d$ -dimensional PDF  $f(x_1, \dots, x_d)$  can be computed. A possible solution is to express Eq. (2) in terms of two-dimensional copulas. The starting point is that  $f(x_1, \dots, x_d)$  can be factorized into the form

$$f(x_1, \dots, x_d) = f(x_d) \cdot f(x_{d-1}|x_d) \cdot f(x_{d-2}|x_{d-1}, x_d) \cdots f(x_1|x_2, \dots, x_d), \quad (4)$$

with  $f(x_k|\mathbf{y})$  the conditional PDF of the random variable  $x_k$  given the vector of random variables  $\mathbf{y}$ . Now, it can be proved (Czado 2019) that

$$f(x_k|\mathbf{y}) = c_{x_k y_j | \mathbf{y}_{-j}}(F(x_k|\mathbf{y}_{-j}), F(y_j|\mathbf{y}_{-j})|\mathbf{y}_{-j}) \cdot f(x_k|\mathbf{y}_{-j}), \quad (5)$$

where  $c_{x_k y_j | \mathbf{y}_{-j}}(\cdot, \cdot)$  is the conditional copula density,

$$F(x_k|\mathbf{y}) = \frac{\partial C_{x_k y_j | \mathbf{y}_{-j}}(F(x_k|\mathbf{y}_{-j}), F(y_j|\mathbf{y}_{-j})|\mathbf{y}_{-j})}{\partial F(y_j|\mathbf{y}_{-j})}, \quad (6)$$

$C_{x_k y_j | \mathbf{y}_{-j}}(\cdot, \cdot)$  is the conditional copula,  $y_j$  is one arbitrarily chosen component of  $\mathbf{y}$  and  $\mathbf{y}_{-j}$  denotes the  $\mathbf{y}$ -vector, excluding this component. The key point is that these conditional PDFs are expressed in terms of two-dimensional copula densities. The same holds for the PDF  $f(x_1, \dots, x_d)$ . For example, in the three-dimensional case it is

$$f(x_1, x_2, x_3) = f_1(x_1) \cdot f_2(x_2) \cdot f_3(x_3) \cdot c_{12}(F_1(x_1), F_2(x_2)) \cdot c_{23}(F_2(x_2), F_3(x_3)) \cdot c_{13|2}(F(x_1|x_2), F(x_3|x_2)|x_2). \quad (7)$$

Actually, the decomposition (4) is not unique since the indices of the variables  $\{x_k\}$  can be permuted. For instance, a decomposition equivalent to (7) is

$$f(x_1, x_2, x_3) = f_2(x_2) \cdot f_1(x_1) \cdot f_3(x_3) \cdot c_{21}(F_2(x_2), F_1(x_1)) \cdot c_{13}(F_1(x_1), F_3(x_3)) \cdot c_{23|1}(F(x_2|x_1), F(x_3|x_1)|x_1). \quad (8)$$

Although the problem of estimating the PDF  $f(x_1, \dots, x_d)$  has been simplified by means of Eqs. (4)-(6), it is still hard to deal with. The conditional copulas  $C_{x_k y_j | \mathbf{y}_{-j}}$  and corresponding densities  $c_{x_k y_j | \mathbf{y}_{-j}}$  are difficult to estimate. For this reason, usually the conditional copula densities are simplified into the form

$$c_{x_k y_j | \mathbf{y}_{-j}}(F(x_k|\mathbf{y}_{-j}), F(y_j|\mathbf{y}_{-j})|\mathbf{y}_{-j}) \approx c_{x_k y_j | \mathbf{y}_{-j}}(F(x|\mathbf{y}_{-j}), F(y|\mathbf{y}_{-j})). \quad (9)$$

Something similarly occurs to the corresponding conditional copulas. This simplification does not only make the problem easier to deal with but, moreover, it permits the use of the large set

of available continuous parametric families of two-dimensional copulas. This makes the method quite flexible. For instance, in the three-dimensional case the decomposition can be written in the form

$$\begin{aligned} f(x_1, x_2, x_3) = & f_1(x_1) \cdot f_2(x_2) \cdot f_3(x_3) \\ & \cdot c_{12}(F_1(x_1), F_2(x_2); \theta_{12}) \cdot c_{23}(F_2(x_2), F_3(x_3); \theta_{23}) \\ & \cdot c_{13|2}(F(x_1|x_2), F(x_3|x_2); \theta_{13|2}), \end{aligned} \quad (10)$$

where the two-dimensional copula densities  $c_{12}(\cdot, \cdot; \theta_{12})$ ,  $c_{23}(\cdot, \cdot; \theta_{23})$  and  $c_{13|2}(\cdot, \cdot; \theta_{13|2})$  can be chosen different.

#### 4. Vine copulas: the theory

For high dimensional distributions, there is a huge number of possibilities for decompositions into two-dimensional copulas, named pair-copulas, like to Eqs. (7) and (8). All these possibilities can be organized by graphical models, called "regular vines". Two special cases, called D-vine and C-vine (Aas et al. 2009), have been introduced as a simplification. Each model gives a specific way of decomposing a density.

Figure 1 shows the graphical structure of a D-vine for a four-dimensional problem. This structure is formed by three levels or trees. Each circle or ellipsis constitutes a node and each pair of nodes is joined by an edge. The label of a node in a given tree is given by the label of the edges of the tree at its immediate left. The label of an edge is given by the indices contained in the joined nodes with the conditional index given by the index common to both. For example, in the central tree the node (1, 2) is connected to the node (2, 3). The common index is 2, hence the label of the joining edge is (1, 3|2). Each edge represents a pair-copula density, and the edge label corresponds to the subscript of the pair-copula density. The indices of the CDFs that appear as the argument of a specific pair-copula density are given by the labels of the nodes connected by the corresponding edge. According to this rule, the first tree produces the terms  $c_{12}(F_1(x_1), F_2(x_2))$ ,  $c_{23}(F_2(x_2), F_3(x_3))$  and  $c_{34}(F_3(x_3), F_4(x_4))$ . The second tree produces the terms  $c_{13|2}(F(x_1|x_2), F(x_3|x_2))$  and  $c_{24|3}(F(x_2|x_3), F(x_4|x_3))$ . Finally, the last tree produces the term  $c_{14|23}(F(x_1|x_2, x_3), F(x_4|x_2, x_3))$ . The decomposition of  $f(x_1, x_2, x_3, x_4)$  is given by the product of these terms:

$$\begin{aligned} f(x_1, x_2, x_3, x_4) = & f_1(x_1) \cdot f_2(x_2) \cdot f_3(x_3) \cdot f_4(x_4) \\ & \cdot c_{12}(F_1(x_1), F_2(x_2)) \cdot c_{23}(F_2(x_2), F_3(x_3)) \\ & \cdot c_{34}(F_3(x_3), F_4(x_4)) \\ & \cdot c_{13|2}(F(x_1|x_2), F(x_3|x_2)) \cdot c_{24|3}(F(x_2|x_3), F(x_4|x_3)) \\ & \cdot c_{14|23}(F(x_1|x_2, x_3), F(x_4|x_2, x_3)). \end{aligned} \quad (11)$$

For a  $d$ -dimensional density  $f(x_1, \dots, x_d)$  this procedure provides the decomposition formula

$$\begin{aligned} f(x_1, \dots, x_d) = & \prod_{k=1}^d f(x_k) \prod_{j=1}^{d-1} \prod_{i=1}^{d-j} c_{i, i+j|1, \dots, i+j-1} \\ & (F(x_i|x_{i+1}, \dots, x_{i+j-1}), F(x_{i+j}|x_{i+1}, \dots, x_{i+j-1})), \end{aligned} \quad (12)$$

where index  $j$  identifies the trees, while index  $i$  runs over the edges in each tree.

Figure 2 shows the graphical structure of a C-vine again for a four-dimensional problem. While in a D-vine no node in any tree is connected to more than two edges, in a C-vine each tree has a unique node, named root node, that is connected to all the

other nodes. The rules for labeling the nodes and the edges is identical to those of the D-vine. For a C-vine, the decomposition formula is

$$f(x_1, \dots, x_d) = \prod_{k=1}^d f(x_k) \prod_{j=1}^{d-1} \prod_{i=1}^{d-j} c_{j, i+j|1, \dots, j-1} (F(x_j|x_1, \dots, x_{j-1}), F(x_{i+j}|x_1, \dots, x_{j-1})). \quad (13)$$

Although in principle the decompositions provided by the C-vines and the D-vines should be equivalent, actually things are different because of the simplification (9). In general, D-vines are often useful when there is a natural ordering of the variables (e.g., by time), whereas C-vines might be advantageous when a particular variable is known to drive the interactions of the other variables. In such a situation, this variable can be located at the root node of the leftmost tree. In many practical applications, however, no a priori information is available which permits to decide which kind of vine to use. As a consequence, the decision has to be based on which model better fits the data.

#### 5. Vine copulas: computational issues

The flexibility of vine copulas complicates the parameter estimation and the model selection. One needs to select the appropriate parametric families for each pair-copula, estimate the parameters, and find a good structure for the vine trees. Gladly, these problems can mostly be solved in separation – per pair-copula, and per tree level.

Recall that a copula  $C_{1, \dots, d}(\mathbf{u})$  is the distribution function of a random variate  $\mathbf{u} = (u_1, \dots, u_d)$ . In what follows we assume that for all variables  $i = 1, \dots, d$ ,  $n$  uniform variates  $\mathbf{u}_k = \{u_{i,k}\}$ ,  $i = 1, \dots, n$ , are available. As mentioned in Sect. 2, these are commonly obtained by transforming the original data  $\{\mathbf{x}_k\}$  by means of  $\mathbf{u}_k = F_k(\mathbf{x}_k)$ .

##### 5.1. Model fitting in the two-dimensional case

We first consider the simpler two-dimensional case. Suppose to have available the variates  $\{(u_{i,1}, u_{i,2})\}$ ,  $i = 1, \dots, n$ , from a parametric copula model  $c_{12}(u_1, u_2; \theta)$ . Then the parameters  $\theta$  can be estimated by maximum-likelihood

$$\hat{\theta} = \arg \max_{\theta} \sum_{i=1}^n \ln c_{12}(u_{i,1}, u_{i,2}; \theta).$$

In practice, since the true copula is unknown, it is necessary to choose a parametric copula density  $c_{12}^{\mathcal{F}_k}(\cdot, \cdot)$  from a set of families  $\{\mathcal{F}_k\}$ ,  $k = 1, \dots, m$ , with  $n_{p_k}$  parameters each. This is commonly done by estimating the parameters  $\hat{\theta}_k$  for each copula density and then by choosing the one with either the lowest Akaike's information criterion (AIC) or the lowest Bayesian information criterion (BIC) where (Czado 2019)

$$\text{AIC}_k = -2 \sum_{i=1}^n \ln c_{12}^{\mathcal{F}_k}(u_{i,1}, u_{i,2}; \hat{\theta}_k) + 2n_{p_k},$$

$$\text{BIC}_k = -2 \sum_{i=1}^n \ln c_{12}^{\mathcal{F}_k}(u_{i,1}, u_{i,2}; \hat{\theta}_k) + \ln(n)n_{p_k}.$$

##### 5.2. Iterating through tree levels

The methods above work for a single pair-copula. It is straightforward to apply them to all pair-copulas in the first tree level

but the same is not true in later tree levels. The reason is that, as it is shown by Eq. (5), the estimate of a  $d$ -dimensional PDF requires the conditional uniform variates  $u_{k|-j} = F(x_k|y_{-j})$  and  $u_{j|-j} = F(y_j|y_{-j})$  which, however, are not directly available.

To solve this issue, suppose for the moment that the tree structure is known and the pair-copulas up to the  $(\ell - 1)$ th tree level have been fit. In the  $\ell$ th tree, pair-copulas have the form  $c_{i,j|D}$ , where  $D$  is a set of  $\ell - 1$  variable indices called *conditioning set*. Then there are always edges with index  $(i, r|D \setminus k)$  and  $(j, s|D \setminus s)$  in the  $(\ell - 1)$ th tree<sup>1</sup>. With the help of the so-called  $h$ -functions,

$$h_{i|r;D}(u_j|u_r) = \int_0^{u_i} c_{i,r|D \setminus r}(t, u_r) dt, \quad (14)$$

and

$$h_{j|s;D}(u_j|u_r) = \int_0^{u_j} c_{j,s|D \setminus s}(t, u_s) dt, \quad (15)$$

it can be shown that  $c_{i,j|D}(\cdot, \cdot)$  is the joint copula density of the random variables

$$u_{i|D} = h_{i|r;D}(u_{j|D \setminus r}|u_{r|D \setminus r}), \quad (16)$$

and

$$u_{j|D} = h_{j|s;D}(u_{j|D \setminus s}|u_{s|D \setminus s}). \quad (17)$$

Here, the point is that the arguments of the  $h$ -functions have the same form of the corresponding conditional uniform variables, but the conditioning set has one index less. Therefore, it is possible to iterate the above equation until  $D = \emptyset$  which corresponds to the first tree, where data are available. Because the pair-copulas  $c_{i,r|D \setminus r}$  and  $c_{j,s|D \setminus s}$  have already been estimated, we can substitute the estimated models in the expressions above. In this way, we can transform data from pair-copulas in one tree into data required for the estimation in the next tree. The analytical form of the  $h$ -function is available for the most common copulas (Joe 1997; Schepsmeier & Stöber 2013).

### 5.3. Finding the tree structure

The remaining question is how to select the right tree structure. For a C-vine, we need to specify which variable serves as root node in every tree. For a D-vine, it is sufficient to specify the order of variables in the first tree. If  $d > 4$ , there are also other structures than D- and C-vines.

To select an appropriate structure, the heuristic proposed by Dissman et al. (2013) can be used. His idea is to capture the strongest dependencies as early as possible in the tree structure. Here, “strength” is defined as the absolute value of Kendall’s  $\tau$  (for the definition of this quantity see appendix. A). We start in the first tree and compute the (empirical) pair-wise Kendall’s  $\tau$  for all variable pairs. Then we choose the tree that maximizes the sum of absolute pair-wise Kendall’s  $\tau$ . We fit pair-copula models for the edges and compute data for the next tree. On these data, we again compute the Kendall’s  $\tau$  for all possible pairs and select the maximum spanning tree<sup>2</sup>. We continue this way, iterating between structure selection, model fitting, and transforming the data until the whole model is fit. A summary of the whole procedure is given in algorithm 1 and implemented in the VineCopula R-package (Nagler et al. 2019).

<sup>1</sup> Symbol  $H \setminus r$  means the set  $H$  minus its element  $r$ .

<sup>2</sup> A spanning tree is a subset of graph, which has all the vertices covered with minimum possible number of edges.

---

### Algorithm 1 Iterative fitting of vine copula models

---

**Input:** Observations  $u_1, \dots, u_d$ .

---

**for** tree levels  $\ell = 1, \dots, d - 1$ :

1. Calculate empirical Kendall’s  $\tau$  values  $\tau_{i,j|D}$  for all possible edges  $e = (i, j | D)$ .
2. Select the spanning tree  $E_m$  maximizing  $\sum_{e \in E_m} |\tau_e|$ .
3. **for all**  $e \in E_m$ :
  - (i) Based on data  $u_{i_e|D_e}, u_{j_e|D_e}$ , fit a copula model  $c_{i_e,j_e|D_e}$  as in Section 5.1.
  - (ii) Compute corresponding  $h$ -functions  $h_{i_e|j_e;D_e}, h_{j_e|i_e;D_e}$  using formulas (14) and (15).
  - (iii) Set
 
$$u_{i_e|D_e \cup j_e} = h_{i_e|j_e;D_e}(u_{i_e|D_e}|u_{j_e|D_e}),$$

$$u_{j_e|D_e \cup i_e} = h_{j_e|i_e;D_e}(u_{j_e|D_e}|u_{i_e|D_e}).$$

**end for**  
**end for**

---

## 6. Application to an experimental set of data

### 6.1. Data set

We make use of the data published in Andreani et al. (2018) and complement the molecular mass values with additional CO(1-0) line data taken at the NRO 45m antenna at Nobeyama (Andreani et al. 2020a,b). The dataset consists of the K-band luminosity,  $L_K$ , the infrared luminosity,  $L_{FIR}$ , the atomic hydrogen mass,  $M_{HI}$ , and the molecular mass,  $M_{H_2}$ , derived from the CO(1-0) line luminosity towards the volume-limited local galaxy sample Herschel Reference survey (HRS) (Boselli et al. 2010). The dataset is extensively described in Andreani et al. (2018) and references therein.

The set of variables has been chosen because they are related to the main overall physical properties of the sample and their relation to the star-formation activity in the galaxies. We aim at investigating the relationship among those properties and at deriving insights into the driving physical mechanism in their interstellar medium.

### 6.2. Data analysis and interpretation

As first step of the analysis, the PDF of each of the quantities  $\log LK = \log_{10} L_K$ ,  $\log LIR = \log_{10} L_{FIR}$ ,  $\log MHI = \log_{10} M_{HI}$  and  $\log MH2v = \log_{10} M_{H_2}$  has been modeled by means of the generalized lambda distribution (GLD) family (Karian & Dudewicz 2011, and references therein). The members of this family are four-parameter PDFs which are known for their high flexibility and the large range of shapes that they can reproduce. The starship method has been adopted to fix the parameters. The reason is that this method finds the parameters that transform the data closest to the uniform distribution, an attractive characteristic when working with copulas. The results of the fit are shown in Fig. 3. After this step, the procedure presented in the previous section has been applied. The results are shown in Tab. 1 and Fig. 4. The original Kendall’s  $\tau$  coefficients in Tab. 1 are related to the strengths of the relation between the quantities without being dependent on the derived margins. This shows that the strongest correlations occur between the far-IR luminosity  $L_{FIR}$

**Table 1.** Sample Kendall's  $\tau$ .

	logLK	logLIR	logMHI	logMH2v
logLK	1.00	0.25	0.03	0.25
logLIR	0.25	1.00	0.49	0.61
logMHI	0.03	0.49	1.00	0.33
logMH2v	0.25	0.61	0.33	1.00

and the gas masses, first molecular  $M_{H_2}$  and then atomic  $M_{HI}$ , while  $L_{FIR}$  is weakly correlated with the near-IR K-band luminosity,  $L_K$ . On the other side, Fig. 4 indicates the type of vine structure selected, specifically a C-vine, and provides the list of pair-copulas singled out for each edge. For each pair-copula, the values of the corresponding coefficients and of the lower and upper tail dependence coefficients are also shown (for the meaning of last two quantities see appendix. B). The Kendall's  $\tau$  (for tree 1) and partial Kendall's  $\tau$  (for tree 2 and 3) associated to each edge are also shown. This last quantity measures the dependence between two variables after the effect of other variables (the common indices of two nodes) has been removed<sup>3</sup>.

These results can be more clearly interpreted by looking at Fig. 5. As explained in Sec. 5, the structure selection algorithm tries to capture the strongest dependencies first. Figure 5 shows a plot of the tree structure labeled with the Kendall's  $\tau$  (for tree 1) and partial Kendall's  $\tau$  (for tree 2 and 3). Here the logLIR quantity has been selected as root node. This means that it is strongly correlated to all other variables and that it drives part of the dependence between the other variables. In the second tree, the effect of logLIR on the dependence between the others has been removed. There is only some weak negative dependence left.

All this can be interpreted with the fact that although from Tab. 1 the quantities  $M_{HI}$  and  $M_{H_2}$  appear positively dependent, such dependence appears to be driven entirely by their dependence on the quantity  $L_{FIR}$ . Once the dependence of  $L_{FIR}$  is removed from the relation with the other quantities the residual relations  $M_{HI}$  with  $M_{H_2}$  and  $L_K$  with  $M_{HI}$  are negatively dependent (albeit this dependence is quite weak). This means that the dependence shown in Tab. 1 is driven entirely by their dependence on  $L_{FIR}$ .

Since  $L_{FIR}$  is dominated by the thermal dust emission heated by FUV photons by massive stars and residing in molecular clouds, cocoons of star formation processes, this result confirms that the physical properties of the galaxies are driven by their star formation.

For completeness we show in Fig. 6 the original data vs. the data simulated from the the estimated four-dimensional joint PDF whose two-dimensional slices are shown in Fig. 7. Figure 6 shows a good agreement between original and simulated data, while Fig. 7 demonstrates the one-to-one relation between the couple of variables.

## 7. Conclusions

In this work a flexible and effective approach to model the relationship among a set of experimental multidimensional quantities has been presented. This approach consists in modeling the

<sup>3</sup> The “partial Kendall's  $\tau$ ” is computed by means of the Kendall's  $\tau$  between the variates  $u_{i|D}$  and  $u_{j|D}$  in Eqs. (16) and (17). It provides a measure of the relationship between  $u_i$  and  $u_j$  when the influence of the variates corresponding to the set  $D$  is removed.

joint probability density function (PDF) of the data by means of a special type of copulas called vine copulas. Classical copulas are functions which contain all of the information on the relationship between two random quantities. Their major limitation is that they are unable to model multidimensional data. Vine copulas overcome this limitation by expressing the joint PDFs as the product of a set of two-dimensional copula densities and the one-dimensional PDFs corresponding to each quantity. In particular, two types of vine copulas have been considered, say the C-vine and the D-vine. This approach makes the estimation of the joint PDFs amenable to a theoretical treatment and feasible from the computational point of view.

We have applied this method to published data on the near-IR and far-IR luminosities and atomic and molecular masses of the Herschel Reference Sample. We find that the far-IR luminosity,  $L_{FIR}$ , is the key player in driving the galaxy properties in this sample. Despite its original selection in the K-band the HRS sample shows that it is  $L_{FIR}$  that plays a fundamental role. Removing its dependence from the other variables, the K-band luminosity, the atomic and molecular masses, it makes clear that the established relation between these latter does not show up any more.

The  $L_{FIR}$  in this sample is dominated by the thermal dust emission heated by FUV photons produced by massive stars in molecular clouds. Our analysis highlights therefore that the star formation activity of these galaxies is the key parameter driving the galaxy evolution.

*Acknowledgements.*

## References

- Aas, K., Czado, C., Frigessi, A., & Bakken, H. 2009, Insurance: Mathematics and Economics, 44, 182
- Andreani, P., Spinoglio, L., Boselli, A. et al. 2014, A&A 566, A70
- Andreani, P., Boselli, A., Ciesla, L. et al. 2018, A&A 617, A33
- Andreani, P., Miyamoto Y., Kaneko H., Boselli, A., Tatematsu K., Sorai K. Vio R., submitted
- Andreani, P., Miyamoto Y., Kaneko H., Boselli, A., Tatematsu K., Sorai K., in preparation
- Balakrishnan, N., & Lai, C.D. 2010, Continuous Bivariate Distributions (New York: Springer)
- Boselli, A., Eales, S., Cortese, L., et al. 2010, PASP, 122, 261
- Czado, C. 2019, Analyzing Dependent Data with Vine Copulas (New York: Springer)
- Durante, F., & Sempì, C. 2016, Principles of Copula Theory (New York: CRC Press)
- Dissmann, J., Brechmann, E.C., Czado, C. and Kurowicka, D., 2013. Selecting and estimating regular vine copulae and application to financial returns. Computational Statistics & Data Analysis, 59, pp.52-69.
- Kotz, S., Balakrishnan, N., & Johnson, N.L. 2000, Continuous Multivariate Distributions Vol. 1 (New York: John Wiley & Sons, Inc.)
- Nagler, T. & Czado, C. 2016, Journal of Multivariate Analysis, 151, 69
- Nagler, T., Schellhase, C., & Czado, C. 2017, Dependence Modeling, 5, 99
- Nagler, T., Schepsmeier, U., Stoeber, J., Brechmann, E.C., Graeler, B., & Erhardt, T. 2019, VineCopula: Statistical Inference of Vine Copulas. R package version 2.3.0. <https://CRAN.R-project.org/package=VineCopula>

- Nelsen, R.B. 2006, *An Introduction to Copulas* (New York: Springer Science + BusinessMedia, Inc.)
- Hofert, M., Kojadinovic, I., Mächler, M., & Yan, J. 2018, *Elements of Copula Modeling with R* (New York: Springer)
- Joe, H. 1997, *Multivariate Models and Dependence Concepts* (Dordrecht: Springer-Science+Business Media)
- Joe, H. 2015, *Dependence Modeling with Copulas* (New York: CRC Press)
- Karian, Z.A., & Dudewicz, E.J. 2011, *Handbook of Fitting Statistical Distributions with R* (New York: CRC Press)
- Lin, C.A., & Kilbinger, M. 2015, *A&A*, 583, A70
- Lin, C.A., Kilbinger, M., & Pires, S. 2016, *A&A*, 593, A88
- Sato, M., Ichiki, K., & Takeuchi, T. 2010, *Phys. Rev. Lett.*, 105, 251301
- Sato, M., Ichiki, K., & Takeuchi, T. 2011, *Phys. Rev. D*, 83, 023501
- Schepsmeier, U., & Stöber, J. 2013, *Statistical Papers*, 55, 525
- Scherrer, R.J., Berlind, A.A., Mao, Q., & McBride, C.K. 2010, *AJ*, 708, L9
- Takeuchi, T.T. 2010, *MNRAS*, 406, 1830
- Takeuchi, T.T., Sakurai, A., Yuan, F.T., & Burgarella, D. 2011, *Earth Planet Space*, 65, 281

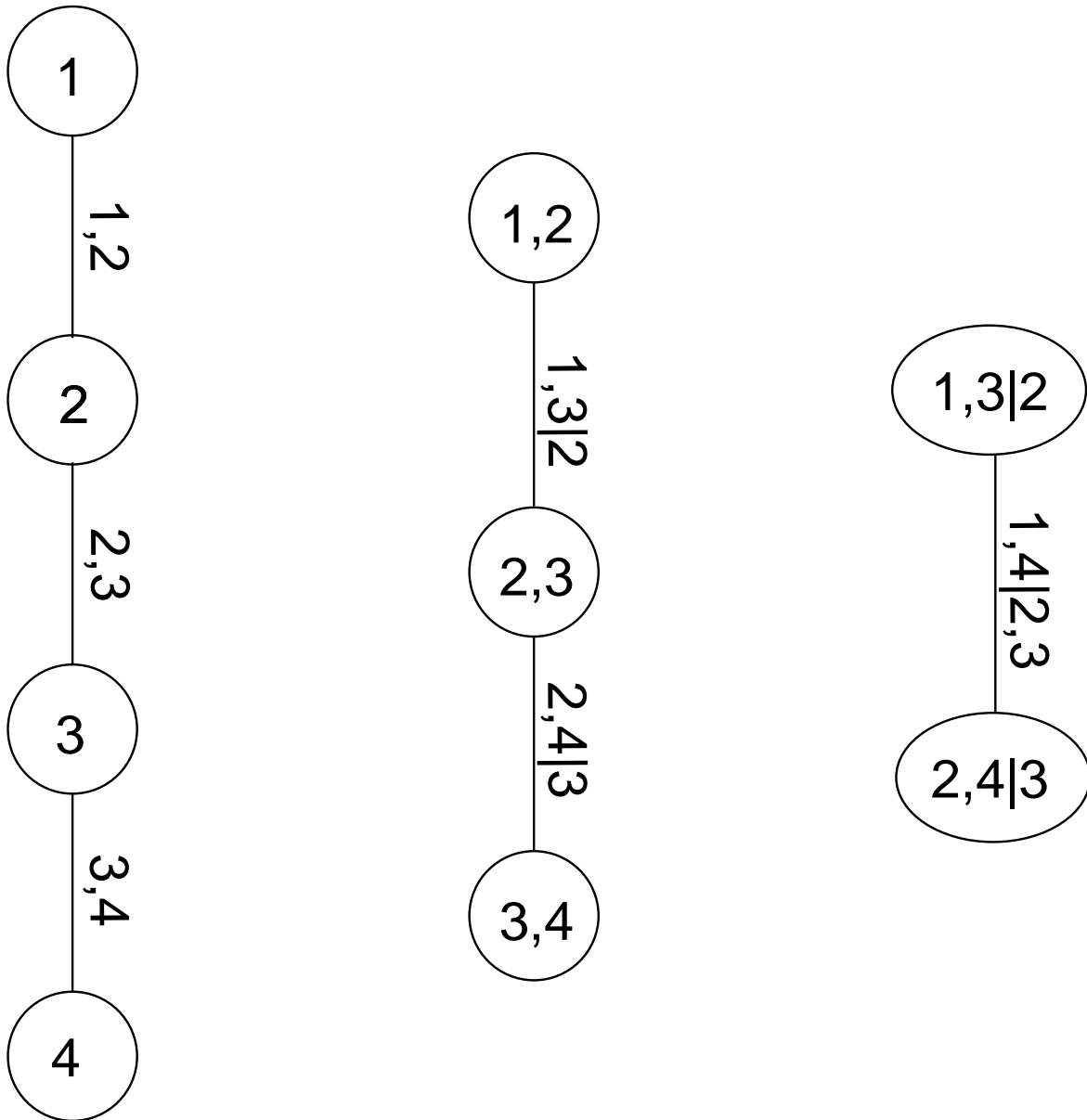


**Fig. 1.** Example of tree structure of a four-dimensional D-vine copula (see text).

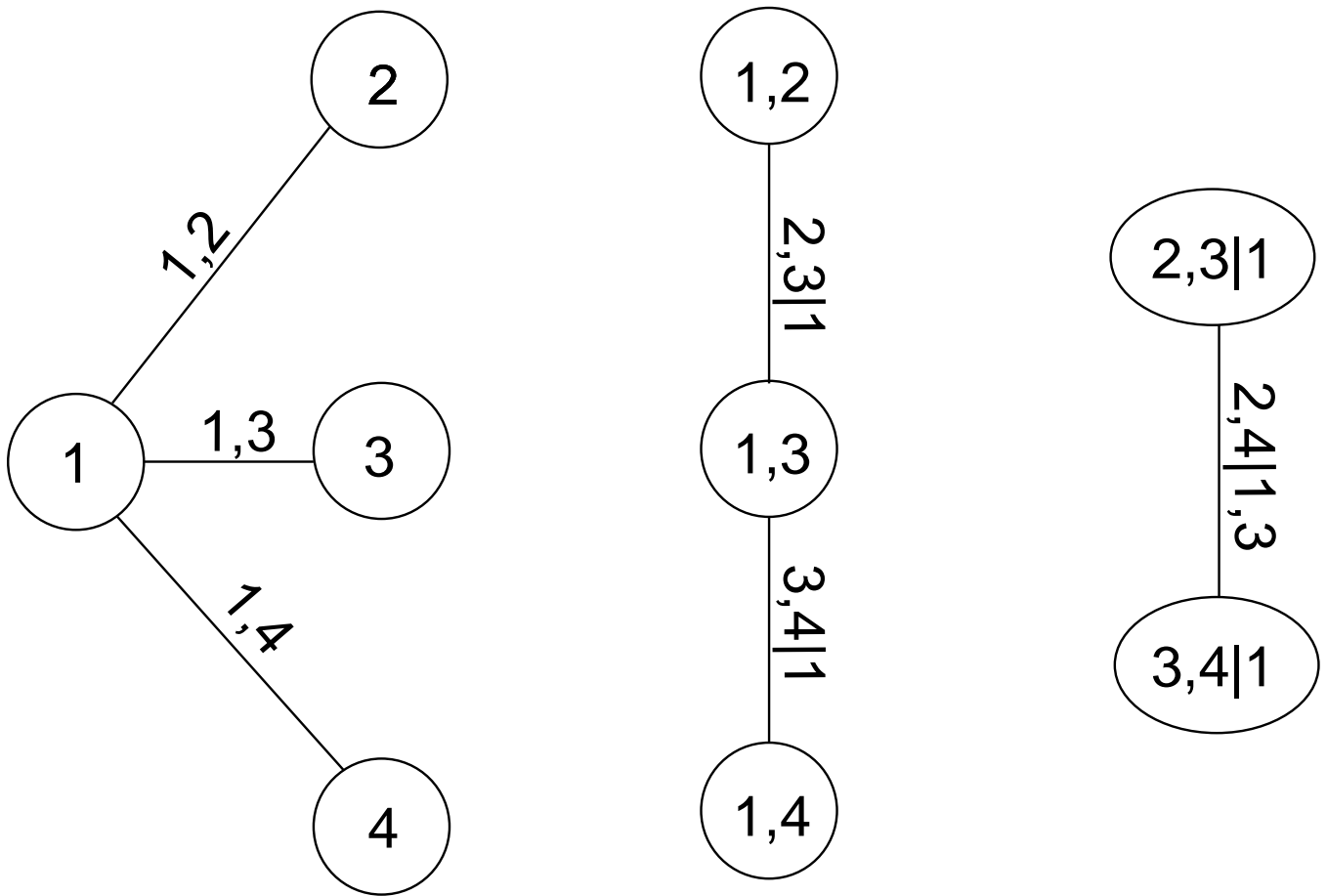


**Fig. 2.** Example of tree structure of a four-dimensional C-vine copula (see text).



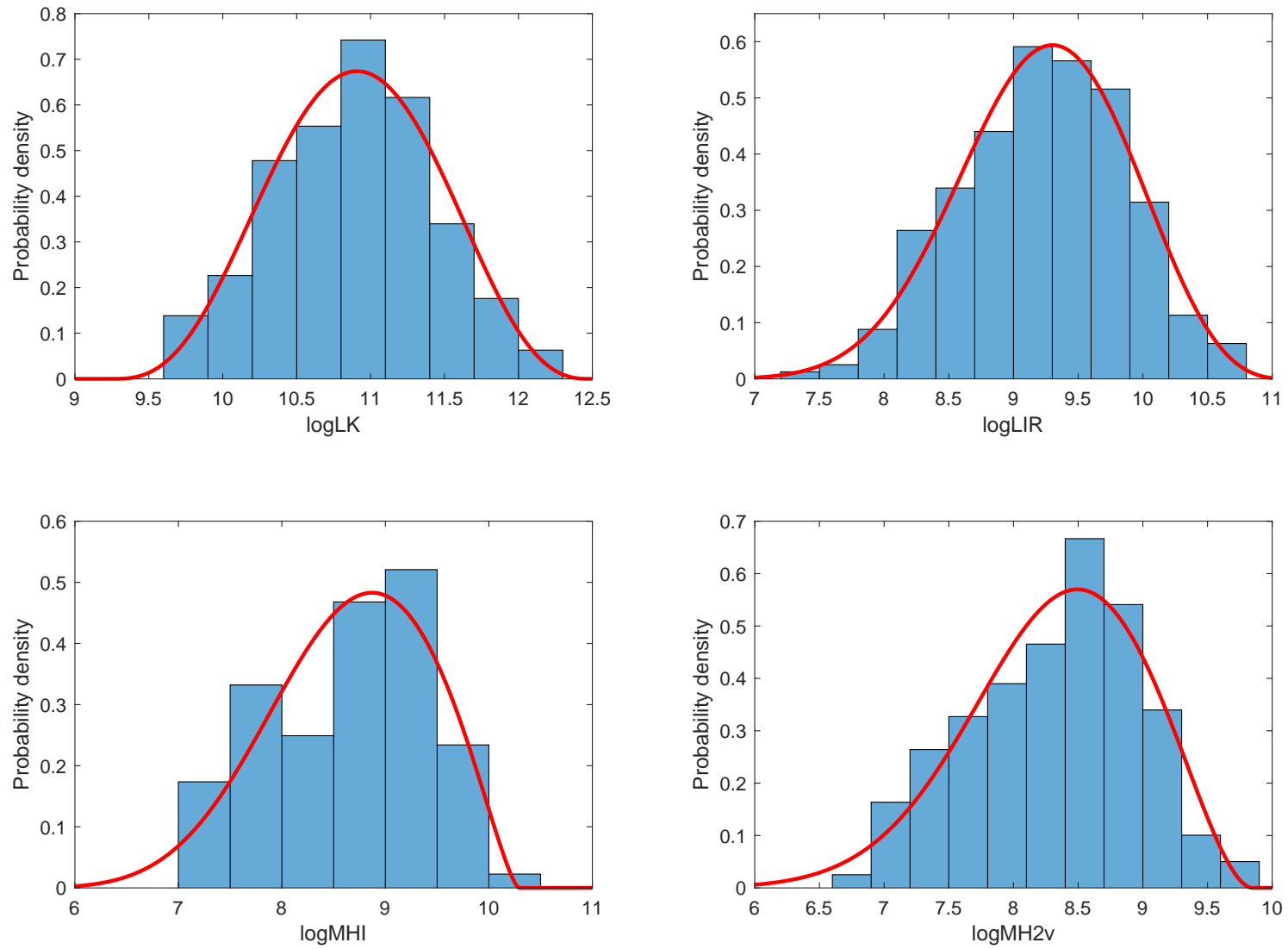


**Fig. 3.** Histograms of the  $\log LK$ ,  $\log LIR$ ,  $\log MHI$  and  $\log MH2v$  data. The red lines provide the PDF obtained by the fit of these data with the generalized lambda distribution family.

tree	edge	copula	par1	par2	tau	utd	ltd
1	2,1	Tawn2	3.31	0.34	0.29	0.33	0
	2,3	Gauss	0.69	0.00	0.49	0	0
	4,2	BB8	4.88	0.92	0.61	0	0
2	3,1 2	BB8_90	-1.66	-0.90	-0.18	0	0
	4,3 2	Frank	-1.02	0.00	-0.11	0	0
3	4,1 3,2	Clayton	0.26	0.00	0.12	0	0.07
type: C-vine							
1 → logLK; 2 → logLIR; 3 → logMHI; 4 → logMH2v							

**Fig. 4.** Results concerning the application of the procedure described in Sec. 5 and 6.2 to the data corresponding to Fig. 3. Here, a copula is associated to each edge as well a Kendall's  $\tau$  for tree 1, a partial Kendall's  $\tau$  for tree 2 and 3 (column "tau") and upper (column "utd"), respectively lower (column "ltd"), tail dependence coefficients. These are theoretical quantities corresponding to the selected copulas whose estimated parameters are given in the columns "par1" and "par2". A description of these copulas can be found in Czado (2019). BB8\_90 means copula BB8 rotated 90°.

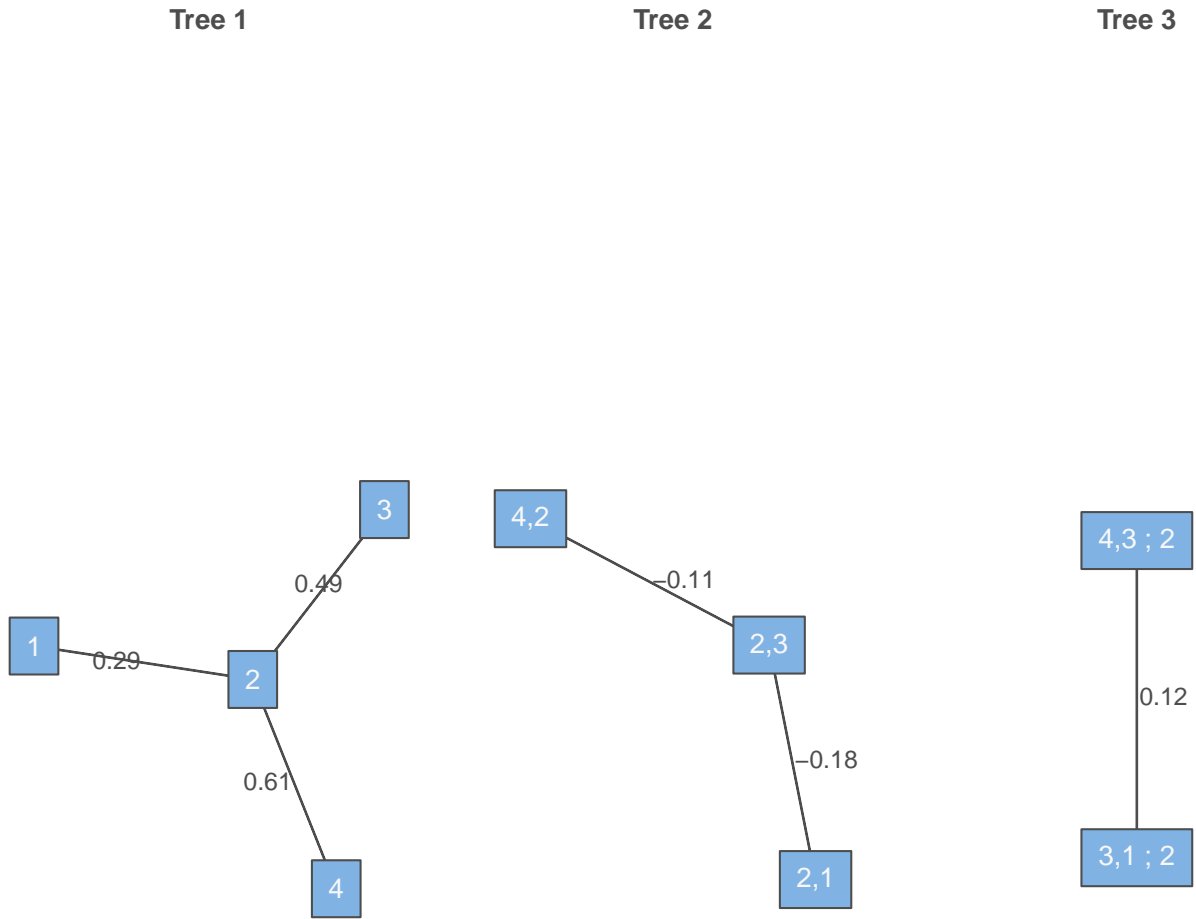


**Fig. 5.** C-vine structure selected by the procedure described in Sec. 5 and 6.2 to the data corresponding to Fig. 3. Each edge in tree 1 is associated to a Kendall's  $\tau$  whereas for tree 2 and 3 to a partial Kendall's  $\tau$  (tau). Here,  $1 \rightarrow \log\text{LK}$ ,  $2 \rightarrow \log\text{LIR}$ ,  $3 \rightarrow \log\text{MHI}$ ,  $4 \rightarrow \log\text{MH2v}$ .

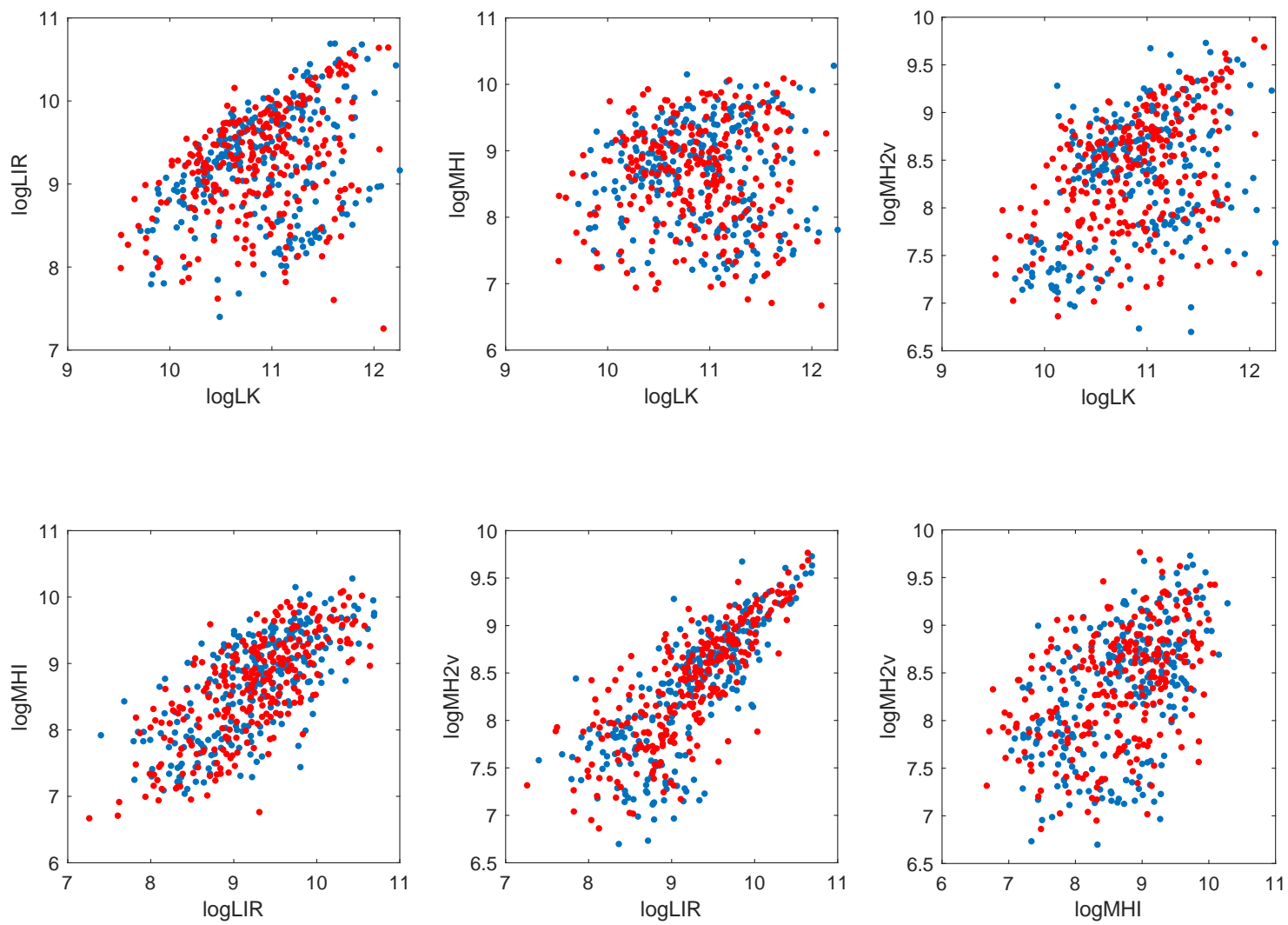


**Fig. 6.** Original  $\log LK$ ,  $\log LIR$ ,  $\log MHI$  and  $\log MH2v$  data (blue circles) vs. the corresponding simulated data obtained from the estimated four-dimensional joint PDF (red circles).

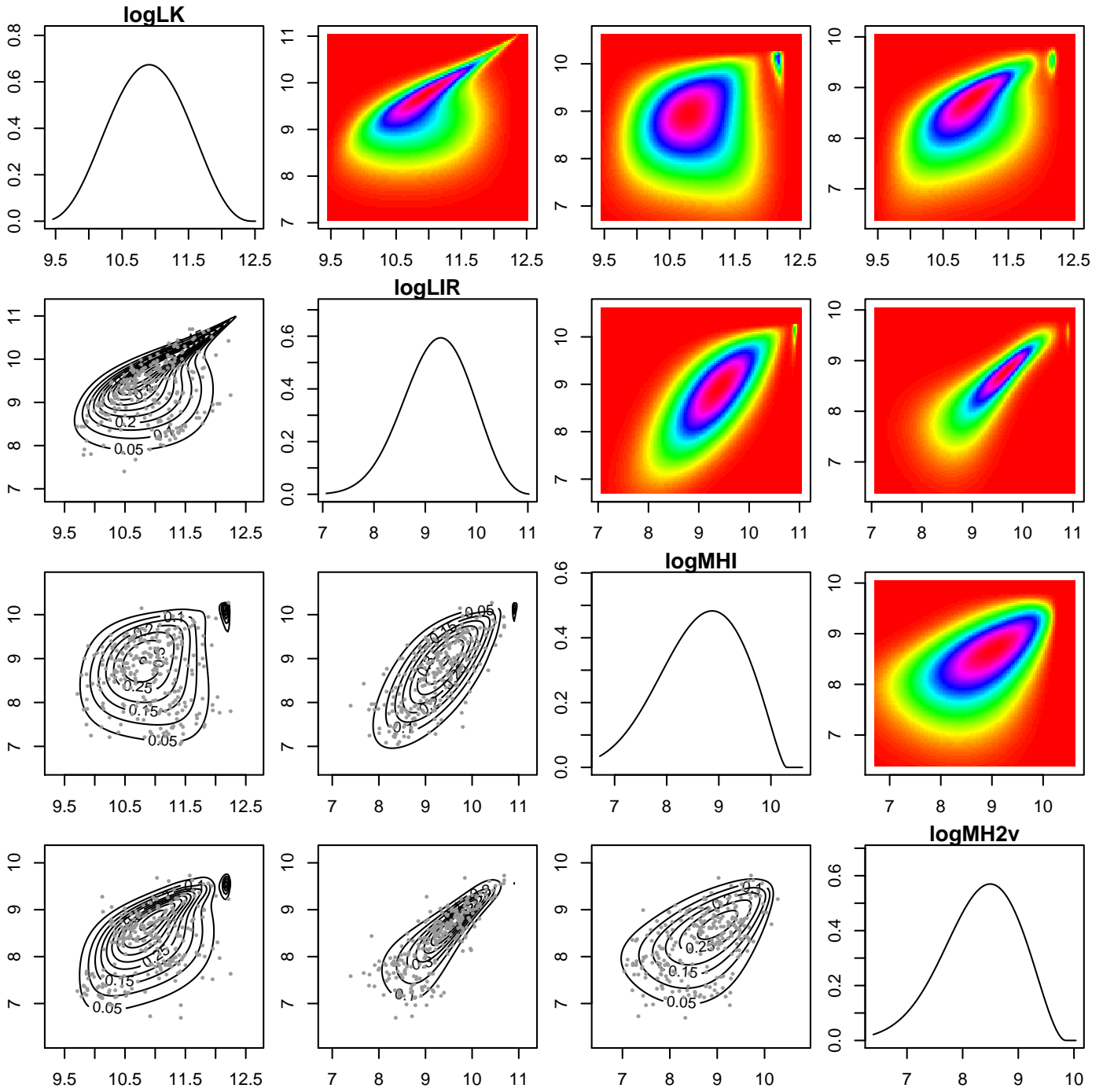


**Fig. 7.** Two-dimensional slices of the estimated four-dimensional joint PDF for the data corresponding to Fig. 3. Along the diagonal are shown the fitted PDFs of Figure 3. The right panels show the slices in which colors correspond to the intensity of the relation, while the left panels report on the same slices the data points and the iso-contours.

## Appendix A: Kendall's $\tau$

When working with copulas the relationship between two random quantities is typically measured by means of the Kendall's  $\tau$ . The reason can be understood by looking at Fig. A.1 which shows the the realization of 1000 independent copies of a bivariate random vector  $(X_1, X_2)$  from the Gaussian, exponential and Cauchy PDFs and of the same number of a bivariate random vector  $(U_1, U_2)$  from the uniform PDF. These realizations appear quite different from one another as well the corresponding linear correlation coefficients  $\rho$ . Here the point is that the first three sets or random numbers  $\{(x_{1,i}, x_{2,i})\}$  have been obtained from the set of uniform random pairs  $\{(u_{1,i}, u_{2,i})\}$  by means of the transformations:

$$(x_1, x_2) = (F^{-1}(u_1), F^{-1}(u_2)), \quad (\text{A.1})$$

where  $F^{-1}(u)$  is the inverse CDF corresponding to the various PDFs. This is a common method to simulate random numbers from a given PDF. What this figure indicates is that the different appearance of the realizations is not due to the intrinsic relationship between the random quantities rather to their margins. Since with copulas one wants to disentangle margins from the dependence structure, the latter should be measured in a way that does not depend on the marginal distributions. This is what the Kendall's  $\tau$  does.

If  $(x'_1, x'_2)$  is an independent copy of  $(x_1, x_2)$ ,  $\tau$  is defined as

$$\tau = \mathbb{P}[(x_1 - x'_1)(x_2 - x'_2) > 0] - \mathbb{P}[(x_1 - x'_1)(x_2 - x'_2) < 0], \quad (\text{A.2})$$

i.e., it is the probability of concordance minus the probability of discordance of the random pairs  $(x_1, x_2)$  and  $(x'_1, x'_2)$ . The rationale behind this definition is that if there is positive dependence between the variable  $x_1$  and  $x_2$ , then when  $x_1$  increases, respectively decreases, a similar behavior has to be expected for  $x_2$ . It can be shown (Hofert et al. 2018) that

$$\tau = 4 \int_0^1 \int_0^1 c(u_1, u_2) C(u_1, u_2) du_1 du_2 - 1, \quad (\text{A.3})$$

i.e.,  $\tau$  effectively depends only on the underlying copula.

The sample version  $\hat{\tau}$  of  $\tau$  is given by

$$\hat{\tau} = \frac{2}{n(n-1)} \sum_{i=1}^{n-1} \sum_{j=i+1}^n \text{sign}[(x_{i1} - x_{j1})(x_{i2} - x_{j2})], \quad (\text{A.4})$$

where  $n$  is the number of observations and  $\text{sign}[x] = 1$  if  $x > 0$ ,  $\text{sign}[x] = 0$  if  $x = 0$  and  $\text{sign}[x] = -1$  if  $x < 0$ . As expected,  $\hat{\tau}$  is the same for all the realizations in Fig. A.1.

## Appendix B: Tail dependence coefficients

There are situations where in the two-dimensional scatterplot of a set of data the points appear concentrated in one or both the tails of their joint distribution. For instance, this is the case for the scatterplots in Fig. A.1 where a concentration of points in the lower-left tail of the joint distribution is evident. Joint distributions characterized by well developed tails indicate a high probability for joint occurrence of extremely small and/or large values. In some practical applications, it is useful to have an estimate of this probability. Given the margins  $F_1(x_1)$  and  $F_2(x_2)$

and the copula  $C(u_1, u_2)$ , the coefficients of lower and upper tail dependence provide such an estimate and are defined as

$$\begin{aligned} \lambda_l &= \lim_{t \rightarrow 0^+} \mathbb{P}(x_2 \leq F_2^{-1}(t) | x_1 \leq F_1^{-1}(t)); \\ &= \lim_{t \rightarrow 0^+} \frac{C(t, t)}{t}, \end{aligned} \quad (\text{B.1})$$

respectively,

$$\begin{aligned} \lambda_u &= \lim_{t \rightarrow 1^-} \mathbb{P}(x_2 > F_2^{-1}(t) | x_1 > F_1^{-1}(t)); \\ &= \lim_{t \rightarrow 1^-} \frac{1 - 2t + C(t, t)}{1 - t}. \end{aligned} \quad (\text{B.2})$$

These coefficients are conditional probabilities which measure the tendency of the random variable  $x_2$  to behave as the random variable  $x_1$ . When their values are close to one it means tail dependence (i.e. high probability of joint extreme values), when close to zero it means tail independence (i.e. small probability of joint extreme values). The analytical expression of  $\lambda_l$  and  $\lambda_u$  is available for various parametric copulas. For instance, the random points in the bottom-left panel of Fig. A.1 have been generated through a Clayton copula with coefficient  $\theta = 5$  for which  $\lambda_l = 0.87$  and  $\lambda_u = 0$ . These values hold also for the other distributions in the same figure.

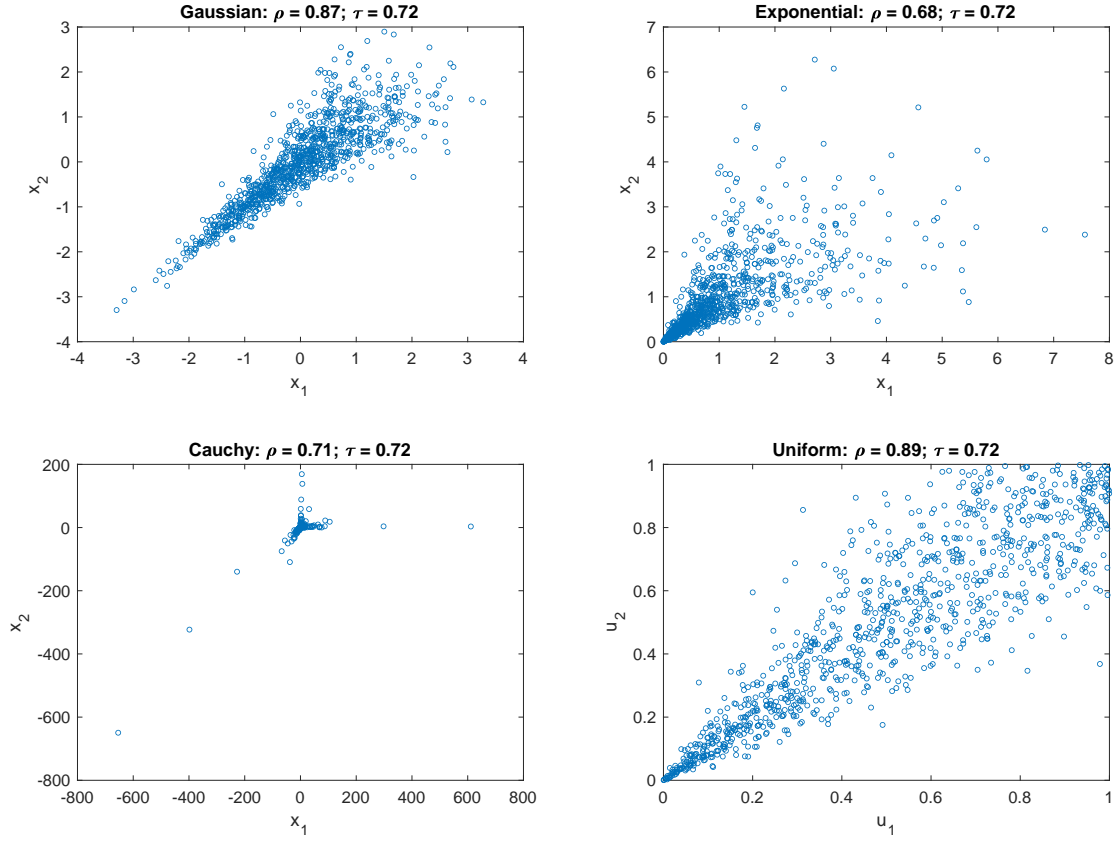


**Fig. A.1.** Numerical realization of 1000 independent copies of a bivariate random vector  $(x_1, x_2)$  from the Gaussian, exponential and Cauchy PDFs obtained from the set of uniform random pairs  $\{(u_{1,i}, u_{2,i})\}$ , shown in the bottom-right panel, by means of the transformations  $(x_1, x_2) = (F^{-1}(u_1), F^{-1}(u_2))$  where  $F^{-1}(u)$  is the inverse CDF corresponding to the various PDFs.